Crystal structures of the cadmium- and mercury-substituted metallo-β-lactamase from Bacteroides fragilis

4 AUTHORS, INCLUDING:

Nestor O Concha
GlaxoSmithKline plc.
29 PUBLICATIONS **1,817** CITATIONS

SEE PROFILE

Karen Bush
Indiana University Bloomington
268 PUBLICATIONS **14,188** CITATIONS

SEE PROFILE

FOR THE RECORD

Crystal structures of the cadmium- and mercury-substituted metallo-β-lactamase from *Bacteroides fragilis*

NESTOR O. CONCHA,[1] BETH A. RASMUSSEN,[2] KAREN BUSH,[2] AND OSNAT HERZBERG[1]

[1]Center for Advanced Research in Biotechnology, University of Maryland Biotechnology Institute, Rockville, Maryland 20850
[2]Wyeth-Ayerst Research, Lederle Laboratories, Pearl River, New Jersey 10965

Abstract: The metallo-β-lactamases require zinc or cadmium for hydrolyzing β-lactam antibiotics and are inhibited by mercurial compounds. To date, there are no clinically useful inhibitors of this class of enzymes. The crystal structure of the Zn^{2+}-bound enzyme from *Bacteroides fragilis* contains a binuclear zinc center in the active site. A hydroxide, coordinated to both zinc atoms, is proposed as the moiety that mounts the nucleophilic attack on the carbonyl carbon atom of the β-lactam ring. To study the metal coordination further, the crystal structures of a Cd^{2+}-bound enzyme and of an Hg^{2+}-soaked zinc-containing enzyme have been determined at 2.1 Å and 2.7 Å, respectively. Given the diffraction resolution, the Cd^{2+}-bound enzyme exhibits the same active-site architecture as that of the Zn^{2+}-bound enzyme, consistent with the fact that both forms are enzymatically active. The 10-fold reduction in activity of the Cd^{2+}-bound molecule compared with the Zn^{2+}-bound enzyme is attributed to fine differences in the charge distribution due to the difference in the ionic radii of the two metals. In contrast, in the Hg^{2+}-bound structure, one of the zinc ions, Zn2, was ejected, and the other zinc ion, Zn1, remained in the same site as in the 2-Zn^{2+}-bound structure. Instead of the ejected zinc, a mercury ion binds between Cys 104 and Cys 181, 4.8 Å away from Zn1 and 3.9 Å away from the site where Zn2 is located in the 2-Zn^{2+}-bound molecule. The perturbed binuclear metal cluster explains the inactivation of the enzyme by mercury compounds.

Keywords: binuclear metal center; cadmium-binding; mercury-binding; metallo-β-lactamase; X-ray structure

β-Lactamases catalyze the hydrolysis of the amide bond of the β-lactam ring typical of antibiotics such as penicillins and cephalosporins, providing the primary mechanism of bacterial resistance to β-lactam therapy. The class B β-lactamases comprise enzymes that require metal ions (zinc, cadmium, cobalt, or man-

ganese) for catalytic activity (Sabath & Abraham, 1966; Davies & Abraham, 1974). There are no clinically useful inhibitors of these metallo-enzymes, although the metal chelators EDTA and 1,10-*o*-phenantroline, and some mercurial compounds have shown inhibitory activity in vitro (Payne, 1993). Recently, a series of mercaptoacetic acid thiol esters have been shown to inhibit some of the enzymes (Payne et al., 1997). Many of the metallo-β-lactamases exhibit broad substrate specificity. For example, the *Bacteroides fragilis* enzyme, the subject of this study, hydrolyzes a wide variety of β-lactam antibiotics with k_{cat}/K_m values on the order of 10^5–10^7 M^{-1} s^{-1} (Yang et al., 1992).

The crystal structure of the metallo-β-lactamases from *B. fragilis* at 1.85-Å resolution revealed a binuclear zinc center in the active site [Concha et al., 1996; Protein Data Bank (PDB) entry code 1ZNB]. The binding of two metals per molecule was also observed by atomic absorption, and the hydrolytic rate toward nitrocefin increased by 2.5-fold when the zinc/protein molar ratio increased from 1 to 2 (Crowder et al., 1996). We have proposed that most, if not all, metallo-β-lactamases function with a binuclear zinc center (Concha et al., 1996), although the enzyme from *Bacillus cereus* functions reasonably well with only one bound zinc (David & Abraham, 1974). The reported low affinity to a second zinc ion (David & Abraham, 1974; Baldwin et al., 1978) and the presence of only one zinc ion in the crystal structure of the *B. cereus* enzyme (Carfi et al., 1995) may be attributed to the use of zinc-chelating buffers. For the *B. fragilis* β-lactamase, the zinc affinity should be at the micromolar range or lower because both sites remain occupied after dialyses from a solution containing 10 μM $ZnCl_2$ to a zinc-free solution (Crowder et al., 1996).

The two zinc ions, termed Zn1 and Zn2, coordinate to six protein residues and two solvent molecules. Zn1 is coordinated in a tetrahedral geometry to three histidines (His 99, His 101, and His 162), and to a solvent molecule that is shared by both zincs. The shared solvent is assumed to be a hydroxide rather than a water molecule because of its electrostatic environment that is dominated by the two cations. Zn2 is coordinated in a trigonal bipyramidal geometry to Asp 103, Cys 181, His 223, the shared hydroxide, and to a second solvent molecule assumed to be a water

molecule. The water molecule and the carboxyl group of Asp 103 occupy the apical coordination positions. We proposed that the metal center prepares a hydroxide for the nucleophilic attack on the carbonyl carbon atom of the β-lactam ring, and that the apical water transfers a proton to the nitrogen atom of the cleaved β-lactam. Zn1 plays an additional role by forming an oxyanion hole with the side chain of the invariant Asn 193. The oxyanion hole helps stabilize the negatively charged tetrahedral intermediate formed during the hydrolytic reaction. Our proposed catalytic mechanism is summarized in Figure 1.

The current study examines further the metal binding to the metallo-β-lactamase from *B. fragilis*. The crystal structures of the Cd^{2+}-bound and the Hg^{2+}-soaked forms have been determined. The kinetic characteristics of the $2Zn^{2+}$-, $2Cd^{2+}$-, and $1Zn^{2+},1Hg^{2+}$-enzymes are rationalized in structural terms.

Results and discussion: *Cadmium-bound metallo-β-lactamase:* Note that the numbering scheme used in this study spans residues 18–249, because the 17 N-terminal amino acid residues comprise a signal peptide that was not included in the expressed protein.

Of the two molecules in the asymmetric unit, the atomic model of molecule A of the Cd^{2+}-bound β-lactamase includes residues 21–44 and residues 51–248. The missing residues, 18–20, 45–50, and 249 are associated with regions of weak electron density map indicative of disorder. Molecule B has also a few disordered residues, and the model includes residues 19–46 and 50–247. Each protein molecule contains two cadmium and one sodium ions. In addition, the model includes 307 water molecules. The crystallographic R-factor is 0.182 for 20,370 reflections in the resolution range 8.0–2.15 Å, for which $F \geq 2 : \sigma(F)$ ($R = \Sigma_h ||F_o| - |F_c||/$

$\Sigma_h |F_o|$, where F_o and F_c are the observed and calculated structure factor amplitudes). The RMS deviations (RMSDs) from ideal bond length and bond angle values of the standard geometry compiled by Engh and Huber (1991) are 0.020 Å and 2.0°, respectively. The electron density at the active site region is shown in Figure 2A. The RMS difference between the α-carbon atom positions of the two molecules in the asymmetric unit is 0.3 Å.

The RMSD of α-carbon atom positions of the cadmium and zinc structures is 0.3 Å. Given the accuracy of X-ray data at 2.15 Å resolution, the cadmium- and the zinc-bound forms of the enzyme have the same structure. The two cadmium ions in molecules A and B are located 3.8 and 3.7 Å apart, respectively, a slight increase over the observed 3.5-Å distance between the two zinc ions (Fig. 2B). The larger Cd^{2+}-Cd^{2+} distance correlates with the larger effective ionic radius of Cd^{2+} compared with the ionic radius of Zn^{2+} (0.95 Å and 0.74 Å, respectively). The cadmium ions exhibit the same coordination pattern as that of the zinc ions: four groups coordinate to Cd1 in a tetrahedral geometry, and five groups coordinate to Cd2 in a trigonal bipyramidal geometry (Table 1). A notable difference between the Cd^{2+}- and the Zn^{2+}-bound enzymes is the distance of the shared hydroxide to the cations. The distance to Cd1 is 1.9/2.1 Å, whereas the distance to Cd2 is 2.4/2.7 Å in molecules A and B, respectively. Because of the resolution limit, caution must be practiced in interpretation of these data, and evaluation of an average distance (2.3 Å) may be more appropriate. Yet again, this value is slightly higher than the distance of the shared hydroxide to the two zinc ions, and, in addition, the shared hydroxide is, within the experimental error, closer to equidistant to the zinc ions (1.9 Å to Zn1 and 2.1 Å to Zn2). Although subtle, such differences may affect catalytic rates.
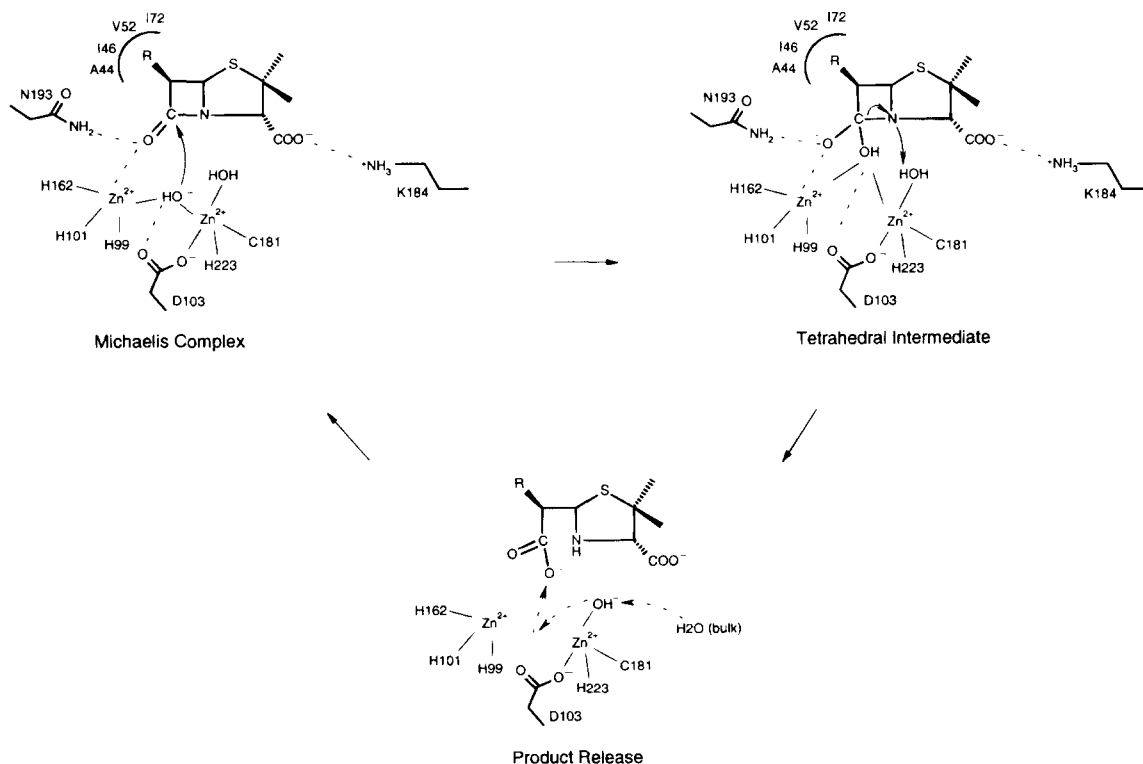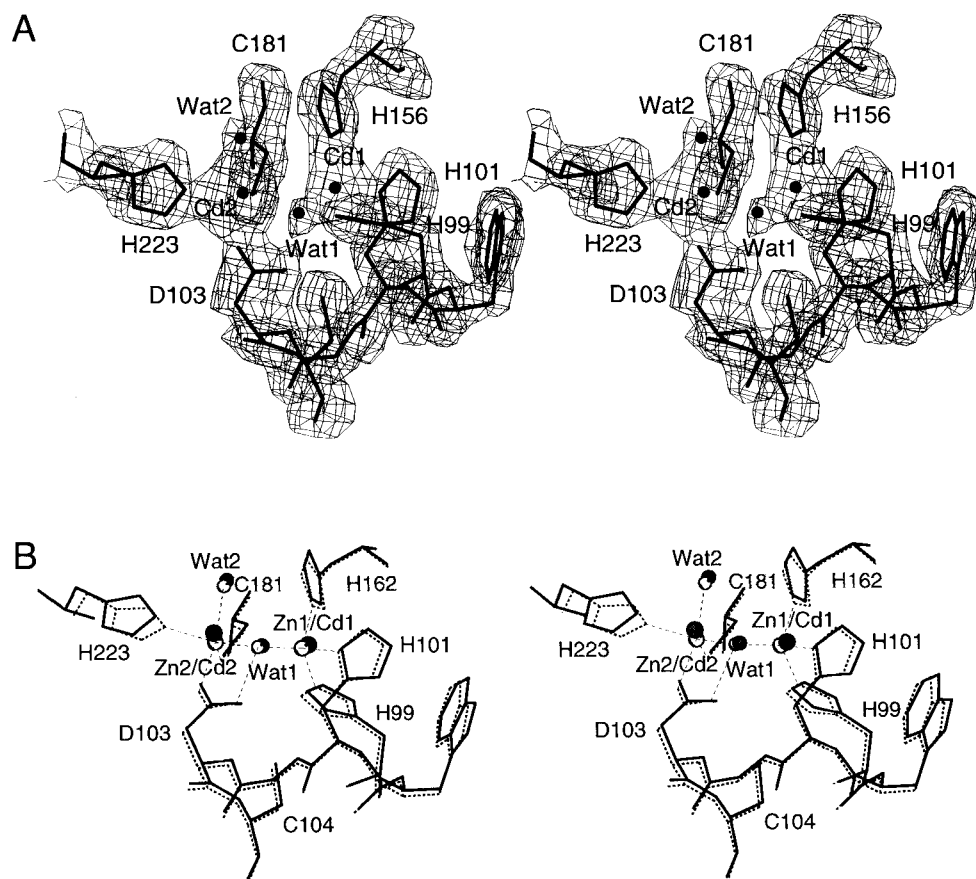

Michaelis Complex

Tetrahedral Intermediate

Product Release

Fig. 1. Proposed catalytic mechanism for the binuclear-center metallo-β-lactamases.

Fig. 2. Active site of the Cd^{2+}-bound crystal structure. **A:** Electron density map at the region of the active site. The coefficients $2F_o - F_c$ and calculated phases are used. The map is contoured at 1σ level. **B:** Superposition of the Cd^{2+} and Zn^{2+} binuclear centers and their environments (solid and broken lines, respectively). Cadmium ions and associated solvent molecules are shown as filled circles, and zinc ions and associated solvent are shown as open circles. Wat 1 corresponds to the hydroxide.

As with the Zn^{2+}-bound form, a sodium ion is bound in the vicinity of the cadmium cluster. It is located underneath the active site depression, 6 Å away from Cd2, with an intervening water molecule between the two cations. We proposed that the sodium ion may play a role in modulating charge distribution during catalysis (Concha et al., 1996). The catalytic apparatus in the Cd^{2+}-bound form remains the same in that respect.

The K_m value for benzylpenicillin hydrolysis by the Cd^{2+}-β-lactamase (93 μM) is twofold larger than that of the Zn^{2+}-bound enzyme (40 μM), whereas the k_{cat} value is one half (81 s^{-1} and 190 s^{-1} for the Cd^{2+}- and Zn^{2+}-bound enzymes, respectively). These values are consistent with previous data that showed that the replacement of Zn^{2+} by Co^{2+} resulted in a 30% decrease in k_{cat}, and less than a threefold increase in the K_m using nitrocefin as substrate (Crowder et al., 1996). Thus, the nature of the metal has only a moderate effect on the catalytic efficiency of the enzyme. The relatively small changes in activity may arise from subtle differences in the electronic structure and ligand configuration of Zn^{2+}, Co^{2+}, and Cd^{2+}, and these in turn may affect the concentration of the nucleophile available for the reaction, and the stabilization of the anionic tetrahedral intermediate.

Mercury-substituted enzyme: Each molecule in the asymmetric unit of the Hg^{2+}-soaked crystal includes all but residues 18–19,

Table 1. *Metal–ligand geometry*[a]

Cd1[b]	(Å)	Cd2[c]	(Å)
A. Cadmium-bound structure			
His 99N$^\epsilon$	2.1/2.3	Asp 1030$^\delta$	2.3/2.2
His 101N$^\delta$	2.1/2.2	Cys 181S$^\gamma$	2.5/2.5
His 162N$^\epsilon$	2.1/2.1	His 223N$^\epsilon$	2.5/2.3
Wat 1/3	1.9/2.1	Wat 1/3^d	2.4/2.7
		Wat 2/4	2.2/2.2

Zn1^c	(Å)	Hg^f	(Å)
B. Mercury-soaked structure			
His 99N$^\epsilon$	2.4/2.3	Cys 104S$^\gamma$	2.3/2.2
His 101N$^\delta$	2.2/2.2	Cys 181S$^\gamma$	2.3/2.5
His 162N$^\epsilon$	2.3/2.4		

[a]Distances to the metal are quated for the two molecules in the asymmetric unit.

[b]Average ligand–Cd1–ligand angle, 109.3°.

[c]Average ligand–Cd2–ligand angles: equatorial (H223N$^\epsilon$, C181S$^\gamma$, Wat 1/3), 118.9°; apex to equatorial (apices: Wat 2/4 and D1030$^\delta$), 90.8°; apex to apex (Wat2/4-Cd-D1030$^\delta$), 167.2°.

[d]Asp 1030$^\delta$–Wat 1/Wat 3 distance, 2.6/2.4 (Å).

[e]Average ligand–Zn1–ligand angle, 93.9°.

[f]Average C$^\beta$-S$^\gamma$-Hg angle, 129.6°; average S$^\gamma$-Hg-S$^\gamma$ angle, 153.9°.

48–49, and 249 that are disordered. In addition, the model includes one zinc, one mercury, and one sodium ion per molecule and a total of 68 water molecules. The crystallographic R-factor is 0.200 for 10,639 reflections in the resolution range 8.0–2.7 Å, for which $F \geq 2\sigma(F)$. The RMSDs from ideal bond length and bond angle values of the standard geometry (Engh & Huber, 1991) are 0.020 Å, and 2.2°, respectively. The electron density map at the active site region is shown in Figure 3A. The RMS difference between the α-carbon atom positions of the two molecules in the asymmetric unit is 0.02 Å. Note that, because of the limited resolution, noncrystallographic symmetry restraints were imposed.

The RMSD in α-carbon atom positions of the Hg^{2+}- and the Zn^{2+}-bound structures is 0.3 Å. Given the limited resolution of the Hg^{2+}-bound structure, the two structures are essentially identical, except for differences around the metal cluster. Although Zn1 and the sodium cations are present, Zn2 has been displaced and a mercury ion occupies an altered site (Fig. 3B). K_2HgI_4 dissociates in the presence of excess KI into HgI_3^- and HgI_2 (Blundell & Johnson, 1976). However, there is no electron density to account for iodine bound to the mercury, and the proximity to the two cysteine residues, Cys 181 and Cys 104, indicates that the reaction proceeded with displacement of the iodine atoms by the sulfhydryl groups of the two cysteine residues.

The mercury ion is located 2.3/2.5 Å from Cys 181 and 2.3/2.2 Å from Cys 104, in molecules A and B, respectively, distances that are consistent with those seen in inorganic crystals (Wells, 1986). The bond angle S^{γ}-Hg-S^{γ} is 154°. The side-chain confor-

mations of both cysteine residues are close to those seen in the 2-Zn^{2+}-bound structure. The Hg^{2+} is located 4.8 Å away from Zn1, and 3.9 Å from the position formerly occupied by Zn2. Zn1 is coordinated to the same histidine side chains as in the 2-Zn^{2+}- and $2Cd^{2+}$- bound structures: His 99, His 101, and His 162.

There is no electron density to account for the shared hydroxide that is present in the Zn^{2+} and Cd^{2+} clusters (Wat 1/3 in Table 1). Because of the limited resolution of the diffraction data, the functional significance of this cannot be assessed. As a control, the difference Fourier map was calculated for the Cd^{2+}-bound crystal at 2.7 Å and 2.1 Å resolutions, omitting the hydroxide from the model. Although a difference peak to account for the hydroxide was clear in the 2.1-Å map, it was missing from the 2.7-Å map. Even if a solvent molecule is present, clearly it cannot mount a nucleophilic attack on β-lactam antibiotics, because mercury binding inhibits the enzymatic activity. The presence of the mercury atom does not change the space available for accommodating substrates in the active site. Inactivation of the enzyme by mercurial compounds is therefore attributed to the binding of the mercury atom in a site that does not overlap with the site of the ejected Zn2, and to the tight binding of the mercury atom to the sulfhydryl group of Cys 181 that leads to disruption of the catalytic apparatus.

Materials and methods: The CcrA3 gene coding for residues 18–249 of the metallo-β-lactamase from *B. fragilis* was expressed in *Escherichia coli* strain BL21 under control of the T7 promoter
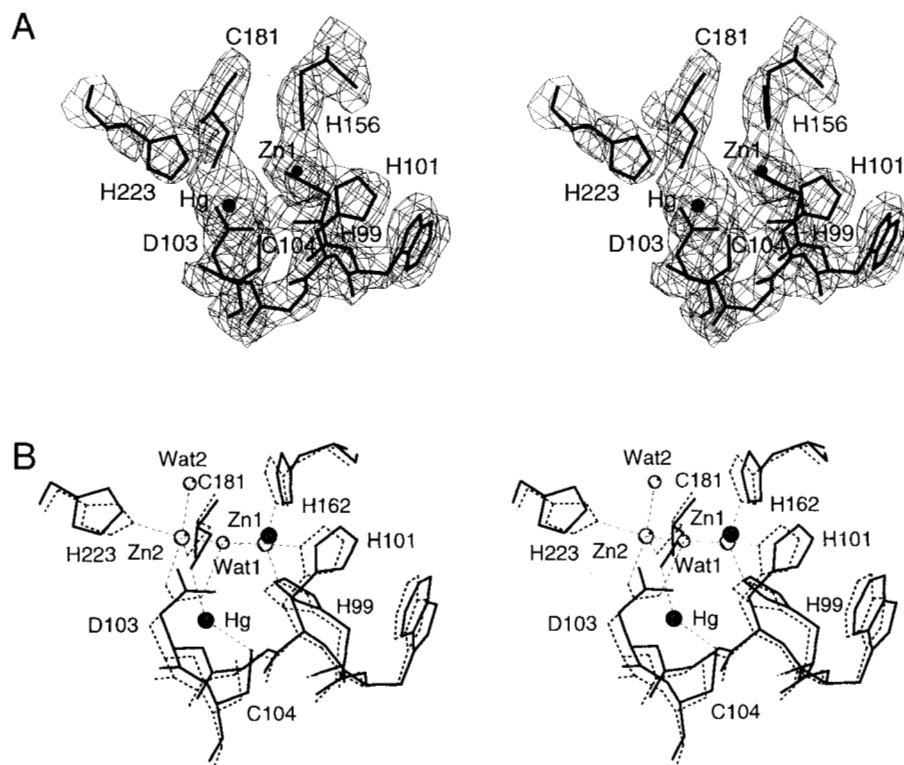
Fig. 3. Active site of the Hg^{2+}-soaked crystal structure. **A:** Electron density map at the region of the active site. The coefficients $2F_o - F_c$ and calculated phases are used. The map is contoured at 1σ level. **B:** Superposition of the Hg^{2+} and Zn^{2+} binuclear centers and their environments (solid and broken lines, respectively). Zinc and mercury ions of the Hg^{2+}-bound structure are shown as open circles, and the zinc ions and associated solvent of the Zn^{2+}-bound structure are shown as open circles. Wat 1 corresponds to the hydroxide.

Table 2. *Crystallographic data and refinement statistics*

	Cd^{2+}	Hg^{2+}
Space group	$P4_32_12$	$P4_32_12$
Cell dimensions (Å)	$a = b = 78.1, c = 139.7$	$a = b = 78.2, c = 140.6$
No. of unique reflections	21,210	11,371
Resolution (Å)	2.15	2.7
Completeness (%)	87.4	90.0
R_{merge}[a]	0.070	0.045
Resolution (Å)	8.0–2.15	8.0–2.71
Unique reflections, $F > 2\sigma(F)$	20,370	10,639
R	0.182	0.200
R_{free}[b]	0.259	0.268
Number of atoms (asymmetric unit)		
Protein	3,387	3,417
Solvent	287	65
Metal	4 Cd^{2+}/2 Na^+	2 Zn^{2+}/2 Hg^{2+}/2 Na^+
RMSD from ideal geometry		
Bond length (Å)	0.02	0.02
Bond angle (°)	2.0	2.2

[a]$R_{merge} = \sum_h \sum_i |\langle I(h) \rangle - I(h)_i|/\sum_h \sum_i I(h)_i$ for equivalent observations.
[b]The R value for 10% of the reflections that were not included in the refinement.

(Yang et al., 1992). The protein was purified from inclusion bodies after solubilization in 8 M urea, and subsequent refolding in the presence of 10–100 μM $ZnCl_2$ or $CdCl_2$ (Rasmussen et al., 1994).

Kinetic assays were performed on a Gilford 250 spectrophotometer at 25 °C in solutions containing 50 mM phosphate buffer, pH 7, and 10 μM of either $ZnCl_2$ or $CdCl_2$. Benzylpenicillin hydrolysis was monitored by loss of absorbance at 240 nm ($\Delta\epsilon_{240} = 540$ M^{-1} cm^{-1}).

Single crystals of the Zn^{2+}- or Cd^{2+}-bound protein were obtained at room temperature by vapor diffusion in hanging drops as described previously (Concha et al., 1996), except that the crystallization solution of the Cd^{2+}-bound form included 10 μM $CdCl_2$ instead of $ZnCl_2$, and 26–28% PEG 2000 instead of PEG 4000. The Hg^{2+}-bound protein crystal was obtained by overnight soaking at room temperature of a Zn^{+2}-bound protein crystal in mother liquor solution containing 10 mM K_2HgI_4 + 20 mM KI.

For data collection, crystals were transferred to solutions of mother liquor containing the respective additives (cadmium or mercury) and 18% glycerol that serves as cryoprotectant (Concha et al., 1996). A single crystal of the Hg^{2+}-bound protein was flash-frozen at approximately 120 K using a modified Enraf-Nonius FR558 liquid nitrogen cryostat. X-ray diffraction data were collected using a Siemens multi-wire area detector mounted on a 3-circle goniostat. Monochromated CuK X-rays were supplied by a Rigaku RU200BH rotating anode operating at 40 kV and 100 mA. Data were processed using XENGEN (Howard et al., 1987). The cadmium data set was collected at the X8C beamline at the National Synchrotron Light Source (Brookhaven National Laboratory, Upton, New York). The data set was obtained from a single crystal that was flash-frozen using an MSC X-Stream Cryosystems. Diffraction intensities were recorded on a charge-coupled device detector mounted on a Huber 4-circle goniostat using 1.000-Å wavelength X-rays. Data acquisition was controlled with the computer program MADNES (Messerschmidt & Pflugrath, 1987). The intensity data were processed with MADNES and PROCOR (Kabsch, 1988). Statistics of data collection are shown in Table 2.

The initial model for the refinement of the two structures was the 1.85-Å refined structure of the Zn^{2+}-bound form (Concha et al., 1996) stripped from solvent molecules and metal ions. The structure provides two crystallographically independent views of the molecule, termed A and B, related to each other by a noncrystallographic rotation axis of 179.6°. The model was refined against diffraction data sets obtained for the Cd^{2+}- and Hg^{2+}-bound protein. The Cd^{2+}-bound structure was refined against data collected from a crystal that was soaked with 1 mM tazobactam for 48 h at room temperature. Tazobactam is a weak inhibitor of the enzyme (Bush et al., 1993). However, no bound adduct could be identified in the difference electron density maps.

The program package XPLOR (Brünger, 1992a) was used for the refinement of the structures. All charges, including those of the metals, were set to zero. The progress of the refinement was evaluated by the quality of the electron density maps and by the reduction of the crystallographic R-factor and the R_{free} values for 10% of the data that were not included in the refinement (Brünger, 1992b). The two molecules in the asymmetric unit were refined independently in the Cd^{2+}-bound structure, but, for the Hg^{2+}-bound structure, the atomic positions were restrained by imposing a 300 kcal mol^{-1} $Å^{-1}$ effective energy constant between the two noncrystallographic symmetry-related molecules. Refinement statistics are shown in Table 2.

References

Baldwin GS, Galdes A, Hill AO, Smith BE, Waley SG, Abraham EP. 1978. Histidines residues as zinc ligands in β-lactamase II. *Biochem J 175*:441–447.

Blundell TL, Johnson LN. 1976. *Protein crystallography*. London, UK: Academic Press.

Brünger AT. 1992a. *X-PLOR version 3.1: A system for X-ray crystallography and NMR*. New Haven, Connecticut: Yale University Press.

Brünger AT. 1992b. Free *R* value: A novel statistical quantity for assessing the accuracy of crystal structures. *Nature 355*:472–475.

Bush K, Macalintal C, Rasmussen BA, Lee VJ, Yang Y. 1993. Kinetic interactions of tazobactam with β-lactamases from all major structural classes. *Antimicrob Agents Chemother 37*:851–858.

Carfi A, Pares S, Duée E, Galleni M, Duez C, Frère JM, Dideberg O. 1995. The 3-D structure of a zinc metallo-β-lactamase from *Bacillus cereus* reveals a new type of protein fold. *EMBO J 14*:4919–4921.

Concha NO, Rasmussen BA, Bush K, Herzberg O. 1996. Crystal structure of the wide-spectrum binuclear zinc β-lactamase from *Bacteroides fragilis*. *Structure 4*:823–836.

Crowder MW, Wang Z, Franklin SL, Zovinka EP, Benkovic SJ. 1996. Characterization of the metal-binding sites of the β-lactamase from *Bacteroides fragilis*. *Biochemistry 35*:12126–12132.

Davies RB, Abraham EP. 1974. Metal cofactor requirements of β-lactamase II. *Biochem J 143*: 129–135.

Engh RA, Huber R. 1991. Accurate bond and angle parameters for X-ray protein structure refinement. *Acta Crystallogr A 47*:392–400.

Howard AJ, Gilliland GL, Finzel BC, Poulos T, Ohlendorf DO, Salemc FR.

1987. The use of an imaging proportional counter in macromolecular crystallography. *J Appl Crystallogr 20*:383–387.

Kabsch W. 1988. Evaluation of single-crystal X-ray diffraction data from a position-sensitive detector. *J Appl Crystallogr 21*:916–924.

Messerschmidt A, Pflugrath JW. 1987. Crystal orientation and X-ray pattern prediction routines for area detector diffractometer systems in macromolecular crystallography. *J Appl Crystallogr 20*:306–315.

Payne DJ. 1993. Metallo-β-lactamases—A new therapeutic challenge. *J Med Microbiol 39*:93–99.

Payne DJ, Bateson JH, Gasson BC, Proctor D, Khushl T, Farmer TH, Tolson DA, Bell D, Skett PW, Marshall AC, Reid R, Gosez L, Combret Y, Marchand-Brynaert J. 1997. Inhibition of metallo-β-lactamases by a series of mercapto-acetic acid thiol ester derivatives. *Antimicrob Agents Chemother 41*:135–140.

Rasmussen BA, Yang Y, Jacobus N, Bush K. 1994. Contribution of enzymatic properties, cell permeability, and enzyme expression to microbiological activities of β-lactams in three *Bacteroides fragilis* isolates that harbor a metallo-β-lactamase gene. *Antimicrob Agents Chemother 38*:2116–2120.

Sabath LD, Abraham EP. 1966. Zinc as cofactor for cephalosporinase from *Bacillus cereus* 569. *Biochem J 98*:11c–13c.

Wells AF. 1986. *Structural inorganic chemistry*. Oxford, UK: Clarendon Press.

Yang Y, Rasmussen BA, Bush K. 1992. Biochemical characterization of the metallo-β-lactamase CcrA from *Bacteroides fragilis* TAL3636. *Antimicrob Agents Chemother 36*:1155–1157.